

Control Strategies of VSC Converter for MTDC Network Transient Studies

Lian Liu, Marjan Popov and Mart van der Meijden

Abstract--The trend of integrating bulk renewable energy sources will require implementation of multi-terminal HVDC (MTDC) networks. Because of its flexible controllability, the technology of VSC (voltage source converter) makes the MTDC network possible, especially with the application of modular multilevel converter (MMC). Unlike conventional point-to-point HVDC networks, a multi-terminal HVDC system has a higher complexity with respect to the control strategies resulting from different control purposes. At present, there is a need to conduct post-fault transient studies for certain research objectives. Thus, this paper analyses the influence of the control strategies of converters on the behavior of MTDC network during normal operation and after fault occurrence. According to the simulated results, converters' responses are investigated in detail. Then, the suitable control strategies for a transient study are proposed. The analysis is performed in PSCAD/EMTDC environment.

Keywords: Electromagnetic transient (EMT), HVDC, modular multilevel converter (MMC), multi terminal HVDC (MTDC), PSCAD/EMTDC, VSC

I. INTRODUCTION

THE HVDC system has been utilized for several decades because of its advantages over traditional AC transmission system, such as the: 1. strengthening the capability of transmitting large amount of power with lower cost and losses; 2. transporting power between separate and/or unsynchronized AC networks; 3. increasing the capacity of existing power grid where additional wires are difficult or expensive to install; 4. making the submarine power transmission with undersea cables possible; 5. providing system operation and interconnection of weak networks without reactive power support. These advantages make HVDC systems a promising option for smart grids. The latest voltage source converter (VSC) is no longer academic research [1] [2] but a commercial product [3] [4] [5].

Currently, HVDC technology has been mainly used for point to point transmission. However, there is an increasing need for implementing multi-terminal HVDC systems

resulting from the integration of renewable generation, the electrification of oil- and gas- platforms from on- and off-shore grids and different electricity markets. A multi-terminal HVDC system is a good option for this issue. Unlike conventional thyristor-based line commutated converter (LCC), the flexible controllability of VSC HVDC system makes it an applicable solution for integrating renewable and distributed energy sources [6] because of its independence in the control of AC voltage and active power. Besides, with the application of pulse-width modulation (PWM) control, AC side filter requirements also decrease.

VSC converters are defenseless against DC faults, because the semiconductors, e.g. IGBTs, GTOs, will be blocked during faults, which leaves anti-parallel diodes (freewheel diodes) to be exposed to faults resulting in high currents [7]-[9]. As the diodes cannot withstand large currents, protection devices are required to act within milliseconds range. Present protection methods, e.g. travelling-wave protection, voltage derivative protection, under-voltage etc., are not suitable for multi-terminal DC systems because of the disability of detecting high-value resistance grounded faults, and the long delay and low liability [10] [11]. Thus, the study on protection schemes for multi-terminal HVDC system should be considered in advance. Importantly, the researching results highly depend on transient studies as they deliver relevant information with regard to the network responses.

Unlike traditional point-to-point HVDC links, the MTDC network can be operated for different purposes due to its high complexity, which means that each converter could work in different modes. Although the control mode of converters will not change the planned power flow of steady state, they will correspondingly change the modelling of other components within the network. In order to evaluate the conditions of each converter after disturbances, this paper discusses the influence of control strategies of the MTDC network. The operation mode of each converter is determined from a certain perspective on system stability, and two feasible control strategies of the whole system are proposed. Among which, Strategy I has protective features: by applying it, the fault could be less influential to the healthy part of the system; additionally, it could be helpful for the full system recovery.

The multi-terminal HVDC benchmark of WG B4 of CIGRE [12] is used to study the influence of control strategies. In this paper, for the efficient modelling in electromagnetic transient software package, the MMC efficient model [13] and time-average model are adopted in a hybrid way.

The project is financially supported by China Scholarship Council (CSC). Lian Liu and Marjan Popov are with the Faculty of EEMCS, Delft University of Technology, Mekelweg 4, 2628 CD Delft, The Netherlands (e-mail: Lian.Liu@tudelft.nl; M.Popov@ieee.org). Mart van der Meijden is with TSO TenneT and the Faculty of EEMCS, Delft University of Technology, Mekelweg 4, 2628 CD Delft, The Netherlands (e-mail: M.A.M.M.vanderMeijden@tudelft.nl).

The paper is organized as follows. In Section II, the configuration of multi-terminal HVDC system are introduced. Then Section III deals with the determination and discussion of control strategies. The simulations and conclusions are provided in Section IV and V respectively.

II. MODELLING OF MULTI-TERMINAL HVDC SYSTEM

A. System Description

At present, there is no commercially available MTDC system, and CIGRE WG B4 proposed a MTDC benchmark as a future vision, which is composed of three DC sub-systems: including two mono-polar systems (DCS1 and DCS2) and one bi-polar system (DCS3).

The established system is shown in Fig.1. The operating voltages of mono-polar and bi-polar VSC-based DC systems are $\pm 200\text{kV}$ and $\pm 400\text{kV}$ respectively, and the limit is from 0.95pu to 1.05pu. The off-shore and on-shore AC systems work at 145 kV and 380 kV respectively. As the focus of this research is on the DC systems, the AC systems are simply modelled with voltage source routines in PSCAD. All the detailed information of these sub-systems can be obtained from [12].

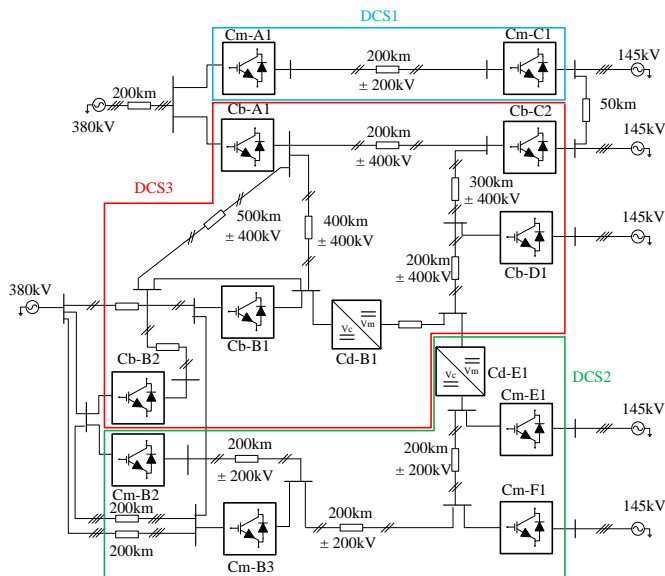


Fig. 1 Configuration of test system

B. Controller

The multi-terminal HVDC system is based on the VSC converter controlled by vector control with decoupled inner current controllers [14]. The vector control strategy calculates a voltage time area across the transformer/converter equivalent reactor, which is required to change the current from present value to the reference value. The dq0-frame current orders to the controller are calculated from set-points or references. Fig.2 shows the complete schematic of the controller. There are also supplementary controllers that can be applied to achieve other control purposes, which are not shown here but will be mentioned in following sections.

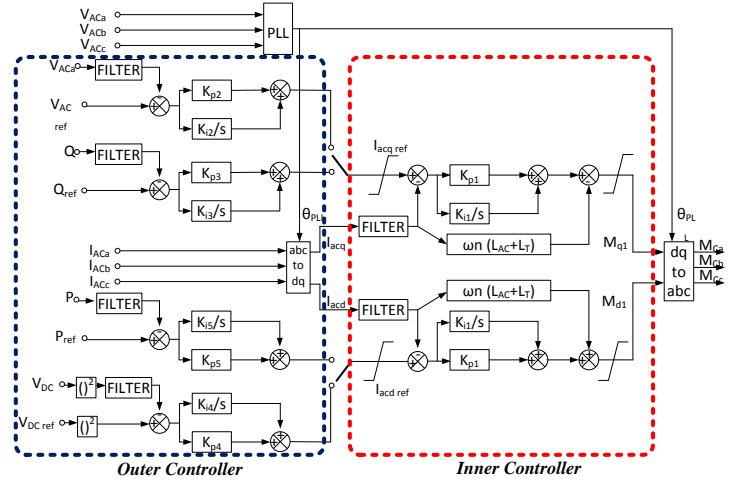


Fig.2 Complete schematic of controller

C. Modelling of AC/DC Converter

This paper applies two methods of modelling AC/DC converter as follows:

1) Time-average model

The time-average model consists of two controlled sources (controlled voltage source and controlled current source), one ideal transformer and four passive elements, as presented in Fig.3. The two controlled sources represent the ideal AC/DC converter that has same apparent power rating with an ideal transformer. The values of four passive elements are selected based on a real project [15]. In DC system, the per-unit values of inductor and capacitor are expressed as time constants in milliseconds, not in percentage. The pole data are tabulated in Table I.

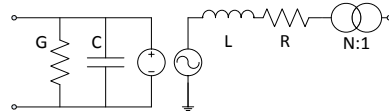


Fig. 3 Topology of AC/DC converter

TABLE I
DATA OF AC/DC CONVERTER

	pu	E1	C2	A1, B2, C1, D1, F1	A1, B1, B2, B3
S	1.0	200MVA	400MVA	800MVA	1200MVA
L	25.50%	196mH	98mH	49mH	33mH
R	1%	2.42Ω	1.21Ω	0.605Ω	0.403Ω
G	0.10%	1.25μS	2.5μS	5μS	7.5μS
C	60 ms	75μF	150μF	300μF	450μF

2) Efficient Model

The MMC converter is the most advanced VSC technology. However, its detailed model is hard for modelling in PSCAD because of its large amount of semi-conductors (GTOs or IGBTs): the nodal matrix has to be inverted in every switching action. Yet according to [13], by using Nested Fast and Simultaneous Solution, the multi-node network of MMC can be modelled with a Thevenin circuit. This model decreases the simulation time and imitates the real operation of semi-conductors. In the following passages, it will be called an efficient model.

Modelling a large system in EMT software takes

considerable amount of time, especially with numerous detailed converter models, yet the time-average model is insufficient for DC transient studies as the behavior of switching components cannot be modelled. Therefore, this system could be modeled in a hybrid way. The specific selection of AC/DC converter model is based on the fault influence on each converter: the converters with obvious transient behaviors against disturbances are modelled with an efficient model while other converters are modelled with time-average model.

D. DC/DC converter

The DC/DC converter is always used to adjust power flow in DC grid especially if there are a large number of AC/DC converters and the whole system control strategy has insufficient margin. A simplified model for a DC/DC converter is shown in Fig. 4 [12]. With four passive elements, the converter consists of a controlled voltage source on low-voltage (LV) side and a controlled current source on high-voltage (HV) side, which are linked by the equation $V_1 I_1 = V_2 I_2$ (supposing a lossless converter). The converter Cd-B1 works at 800kV on both sides, while Cd-E1 works at 800kV on HV side, 400kV on LV side. It should be noticed that this DC/DC converter can only achieve one-directional power delivery from HV to LV. The parameters of four passive elements are listed in Table II.

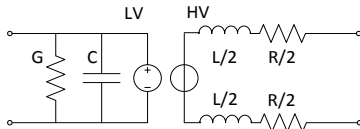


Fig.4. Simplified DC/DC converter

TABLE II
DATA OF DC/DC CONVERTER

	pu	E1	B1
S	1.0	1000MW	2000MW
L	5ms	800mH	1600mH
R	1.20%	1.92Ω	3.84Ω
G	0.025%	0.390625μS	0.78125μS
C	5ms	7.8125μF	15.625μF

E. Transmission Line System

Although the underground or submarine cables are seldom short-circuited when compared with OHL (overhead line), it is a critical condition for DC lines that needs analyzing. Therefore, for a large scale HVDC system, especially a multi-terminal HVDC system, detailed and appropriate modelling of dc cable is necessary for accurate transient analysis.

Four kinds of transmission line models are available in PSCAD/EMTDC. Among which, it is decided to use Frequency Dependent (Phase) Model [16] for the simulation in order to capture the wave front after disturbance, as it is basically a distributed RLC travelling wave model with the highest accuracy. The configuration of coaxial cable in PSCAD is shown in Fig.5. Detailed cable physical data and underground environment data can be found in [17]. The parameters are listed in Table III.

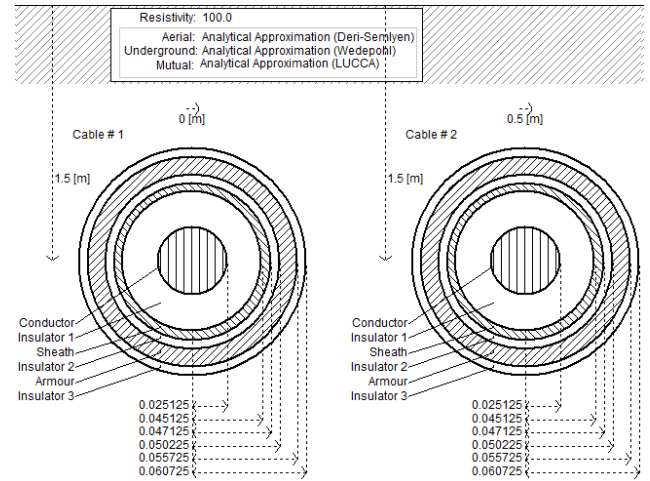


Fig.5 Coaxial cable model in PSCAD

TABLE III
DATA OF CABLE MODEL

Layer	Material	Outer diameter (mm)	Resistivity (Ω·m)	Relative permittivity	Relative permeability
Core	Copper	25.125	1.72E-08	1	1
Insulation	XLPE	20	-	2.3	1
Sheath	Lead	22	2.20E-07	1	1
Insulation	XLPE	25.1	-	2.3	1
Armor	Steel	30.6	1.80E-07	1	10
Insulation	PP	35.6	-	2.1	1

III. POSSIBLE CONTROL STRATEGIES

In this section, two system control strategies are proposed. For the convenient comparison, the power flows in each strategy are same.

A. MTDC Connecting Infinite Buses

As Fig. 1 shows, the system consists of four independent 145kV AC systems (lower-voltage systems). When dealing with the control modes of converters connecting them, it depends on the properties of these systems. Thus, it is firstly assumed that all these lower-voltage systems are AC systems with infinite capacity, which have high inertia and short circuit ratio (SCR). Then System C (Cm-C1 and Cb-C2), D (Cb-D1) and F (Cm-F1) can operate at their rated voltage and the load on System E (Cm-E1) can be regarded as electrification of an oil platform. Based on this assumption, the converter Cm-C1, Cb-C2, Cb-D1 and Cm-F1 work at rectifier mode, importing power into DC network.

In each DC sub-system, there should be at least one converter working as a slack bus, which takes the responsibility of maintaining DC voltage that determines the power flow between terminals. This slack-bus converter should be connected to a strong AC system. In DCS1, only converter Cm-A1 can be a DC voltage regulator. At the same time, the DCS2 is a four-terminal network, which links DCS3 through a DC/DC converter Cd-E1. It has been verified that either Cm-B2 or Cm-B3 can be a DC regulator. The set point of DC voltage reference could be from 0.99pu to 0.98pu, when taking power flow and lose into consideration.

Because of the meshed network topology and two DC/DC converters, the DCS3 is the most complex sub-system. As the converter Cb-C2, Cb-D1 have been decided to control the real power of DC network, one of Cb-A1, Cb-B1 and Cb-B2 should control the DC voltage. According to the proposed power flow in [12], it can be observed that the power is mainly delivered into AC system through Cb-B1 and Cb-B2, so it is advisable to set them as inverters controlling real power and run Cb-A1 as a slack bus.

Unlike conventional two terminal HVDC, which is straightforward on power balancing, in a complex DC network, there are many rectifiers supplying power to DC grid and also many inverters drawing power from the grid. It is acceptable that some inverters draw fixed DC power, as the load on conventional AC grids. As mentioned before, the power flow is determined by the voltage differences between each terminal. A power imbalance will result in DC voltage excursion, which is similar to the frequency fluctuation on AC grids. Therefore, in order to ensure power balancing and dynamical support DC network stability and transient responses, it is advisable for rectifiers or inverters operating in power control where the power references are automatically adjusted with DC voltage variation according to (1), in which p_{ref} is the new real power reference, p_{ref_set} and u_{DC_set} are the original set points, u_{DC} represents measured DC voltage. The reliability of the dc grid can be significantly enhanced by DC voltage droop control since multiple converters can simultaneously contribute to the dc voltage stability. If only a small contribution for balancing purpose is required, the deadband control can be adopted. However, according to the simulation results, the droop control is enough.

$$p_{ref} = p_{ref_set} + (u_{DC} - u_{DC_set}) / k_{droop_DC} \quad (1)$$

Besides the capability of supporting DC network, the converters are considered to support AC grid by using the q-axis current order. Especially for the converters in inverter mode, they should be treated as a conventional power plant and it is acceptable to use generators control the re-active power with AC voltage droop feedback. Similarly, the re-active power is regulated based on (2). As another option, the AC grid can be supported by active power changed with frequency deviation.

$$q_{ref} = q_{ref_set} + (u_{AC} - u_{AC_set}) / k_{droop_AC} \quad (2)$$

For the AC bus linked two converters, only one of them needs to have Vac droop controller. Thus, the Cb-A1, Cb-B1, Cb-B2 and Cm-B3 are reactive power regulators with AC voltage droop to support AC grid. There is no need for the DC/DC controllers to regulate power flow as it is determined by the AC/DC converters. The DC/DC converters are now acting as DC hubs that maintain the system voltages, thus they are modelled with ideal transformer component in PSCAD. The control Strategy I is listed in Table IV. The reference of active power is from DC side to AC side for the AC/DC converters, while from HV side to LV side for DC/DC converters.

As all the converters take partial responsibility of stabilizing the system, the redundancy of control of this strategy is high. What is more, the high level redundancy gives this strategy a certain level of protective features, which is clarified in Section IV.

TABLE IV
SYSTEM CONTROL STRATEGY I
a) Control Strategy of DCS1

Converter	Control Mode	
	Setpoint	
Cm-A1	Q	Vdc
	$Q=0$	$Vdc=1pu$
Cm-C1	Q(Vac)	P(Vdc)
	$Q=0(Vac=1pu)$	$P=-400MW(Vdc=1pu)$

b) Control Strategy of DCS2

Converter	Control Mode	
	Setpoint	
Cm-B2	Q	Vdc
	$Q=0$	$Vdc=0.99pu$
Cm-B3	Q(Vac)	P(Vdc)
	$Q=0(Vac=1pu)$	$P=800MW$
Cm-E1	Islanded	
Cm-F1	Q(Vac)	P(Vdc)
	$Q=0(Vac=1pu)$	$P=-500MW(Vdc=1pu)$

c) Control Strategy of DCS3

Converter	Control Mode	
	Setpoint	
Cb-A1	Q(Vac)	Vdc
	$Q=0(Vac=1pu)$	$Vdc=1.01pu$
Cb-B1	Q(Vac)	P(Vdc)
	$Q=0(Vac=1pu)$	$P=1500MW(Vdc=1pu)$
Cb-B2	Q(Vac)	P(Vdc)
	$Q=0(Vac=1pu)$	$P=1700MW(Vdc=1pu)$
Cb-C2	Q(Vac)	P(Vdc)
	$Q=0(Vac=1pu)$	$P=-600MW(Vdc=1pu)$
Cb-D1	Q(Vac)	P(Vdc)
	$Q=0(Vac=1pu)$	$P=-1000MW(Vdc=1pu)$

B. MTDC Connecting Offshore Power Plants

These lower-voltage systems can be also treated as wind farms with limited SCR and inertia which are operated at their permitted power generation.

Under this assumption, the converters connecting these wind plants should provide AC voltage and frequency for them, otherwise the power cannot be injected into DC network. Thus, converter Cb-D1, Cm-E1 and Cm-F1 have to be working in islanded mode. For the System C (Cm-C1 and Cb-C2), there is no need for two converters supporting island systems or the two converters will conflict on regulating the AC offshore system, so converter Cm-C1 is selected to be in islanded mode while other converters remain in the same modes as that of Strategy I. The Table V shows the Strategy II.

It is obvious that this strategy has a lower level in control flexibility than Strategy I as the islanded converters cannot participate in regulating the DC network. This strategy, however, is more realistic than Strategy I, as there is a high possibility that the lower-voltage power plants have limited power capacities, low SCR and inertia.

TABLE V
SYSTEM CONTROL STRATEGY II
a) Control Strategy of DCS1

Converter	Control Mode	
	Setpoint	
Cm-A1	Q	Vdc
	$Q=0$	$Vdc=1pu$
Cm-C1	Islanded	

b) Control Strategy of DCS2

Converter	Control Mode	
	Setpoint	
Cm-B2	Q	Vdc
	$Q=0$	$Vdc=0.99pu$
Cm-B3	Q(Vac)	P(Vdc)
	$Q=0(Vac=1pu)$	$P=800MW(Vdc=1pu)$
Cm-E1	Islanded	
Cm-F1	Islanded	

c) Control Strategy of DCS3

Converter	Control Mode	
	Setpoint	
Cb-A1	Q(Vac)	Vdc
	$Q=0(Vac=1pu)$	$Vdc=1.01pu$
Cb-B1	Q(Vac)	P(Vdc)
	$Q=0(Vac=1pu)$	$P=1500MW(Vdc=1pu)$
Cb-B2	Q(Vac)	P(Vdc)
	$Q=0(Vac=1pu)$	$P=1700MW(Vdc=1pu)$
Cb-C2	Q(Vac)	P(Vdc)
	$Q=0(Vac=1pu)$	$P=-600MW(Vdc=1pu)$
Cb-D1	Islanded	
Cd-B1	$P=600MW$	
Cd-E1	$P=300MW$	

IV. COMPARISON OF STRATEGIES AFTER DISTURBANCE

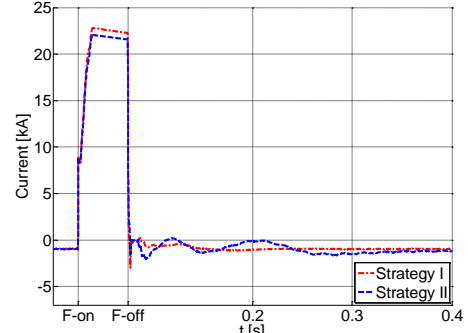
In this section, Strategies I and II will be compared on the transient behaviors of the network during fault and changing network topology.

A. DC Fault at Cm-A1

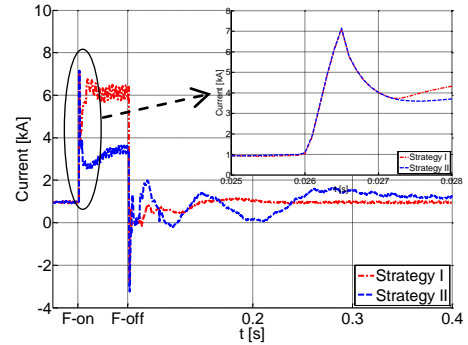
The pole-to-pole fault is the most severe situation in DC system, thus it is worthy of simulation. Thus the fault is applied at the end of converter Cm-A1, starting at 0.025s. Its duration and fault resistance is 50ms and 0.01ohm respectively. The converter will be blocked if the DC current exceeds pre-specified threshold and each converter can be considered separately due to the change of topology during fault. In order to enhance the computation efficiency, the converter Cm-A1 and Cm-C1 are modelled with MMC efficient model while the rest are modelled by using time-average model.

From Fig.6(a), the waveforms of DC terminal currents of Cm-A1, I_{dcCmA1} , are quite similar with each other under two strategies. Because of the fault occurring at the terminal of Cm-A1 and the infinite AC bus BaA0, the DC voltage at this terminal drops to zero immediately, as Fig.7(a) shows. On the other hand, the real power injected through converter CmA1 is determined by the fault characteristic when the converter is blocked and it is irrelevant with AC side, which is clarified by Fig.8(a): the power through CmA1 has good agreement during the fault (from F-on: 0.025s to F-off: 0.075s) with two

strategies.

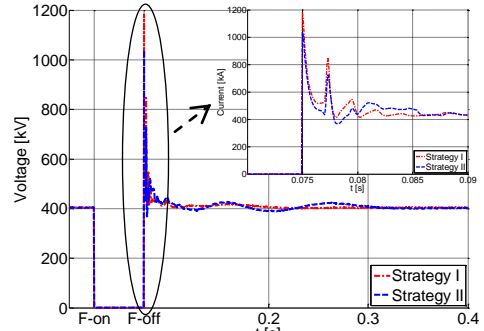


(a)

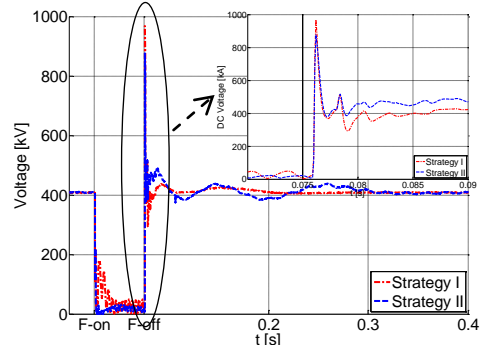


(b)

Fig 6. The DC current at converter terminal: (a)CmA1; (b)CmC1. F-on: 0.025s, F-off: 0.075s.



(a)



(b)

Fig 7. The DC voltage at converter terminal: (a) Cm-A1; (b) Cm-C1. F-on: 0.025s, F-off: 0.075s.

The waveforms of currents I_{dcCmC1} of converter Cm-C1 during fault are quite different under two control strategies, as it is shown in Fig.6(b). It is obvious that there is a spike

around 0.0265ms (fault applied at 0.025s). It occurs because of the arrival of surge travelling from converter CmA1 terminal. Additionally, under Strategy II, the fault current is limited when the converter CmC1 is blocked; there is no AC voltage and frequency provided for the islanded system, thus the power is cut off from System C1 and the injection through Cm-C1 decreases dramatically, as depicted in Fig.8(b). However, the System C1 is linked to an infinite bus under Strategy I, which provides AC voltage and frequency, so even when the converter is blocked and works as an uncontrolled rectifier, the power can still go through. The power is then determined by the configuration of DC network during fault, i.e. transmission line parameters and fault resistance. Therefore, the DC voltage of converter Cm-C1 under Strategy I oscillates during the fault but it is close to zero under Strategy II as Fig. 7(b) demonstrates.

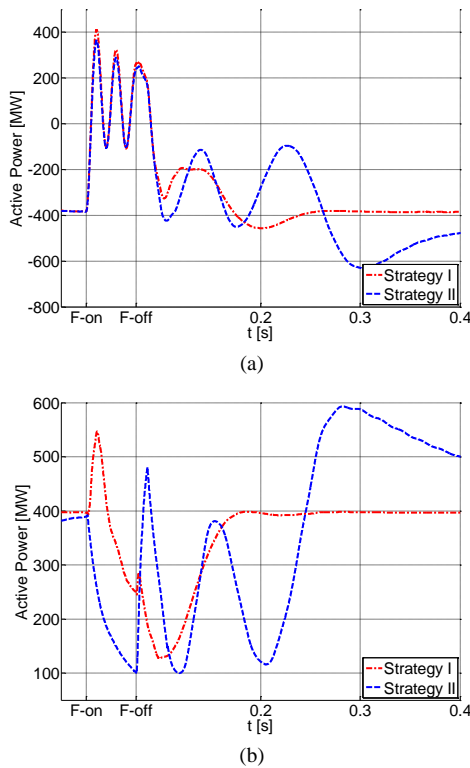


Fig 8. The imported power through converter: (a) Cm-A1; (b)Cm-C1. F-on: 0.025s, F-off: 0.075s.

After the fault is cleared at F-off: 0.075s, the system recovers differently under two strategies. The DC voltage of sub-system DCS1 is regulated by converter CmA1 and it can be stable again only with several negligible fluctuation no matter applying Strategy I or II. However, it can be seen that Strategy I is much more efficient than Strategy II in regulating active power injection into the HVDC grid, as it is shown in Fig. 8(a) and (b): when the fault is removed from the grid at the instant of F-off, the power can stabilize within 0.125s ($\sigma = \pm 5\%$), and the overshoots are only around 15.5% and 1.5% respectively for converter Cm-A1 and Cm-C1 under Strategy I. However, the stable time and overshoot for Strategy II are longer and larger than those of Strategy I, which are 0.505s

($\sigma = \pm 5\%$) and 58% for converter Cm-A1, 0.555s ($\sigma = \pm 5\%$) and 48.25% for Cm-C1. Considering that the DC voltages have similar patterns under both strategies, the current of DC network of Strategy I can restore to pre-fault level faster than Strategy II.

B. Switching Off and On Cable A1-C2

Because of the flexibility of multi-terminal DC system, one or more cables could be switched off because of faults or maintenance purposes, so this situation is also considered here.

The cable connecting DC bus Bb-A1 and Bb-C2 is switched off and on at S-off: 0.025s and S-on: 0.225s respectively. The power flows of DCS3 with two strategies are shown in Fig.9.

The reaction of each DC sub-system can be observed from Fig.10 to Fig.12. For the easy discrimination, the DC current references of Cm-A1 and Cm-C1 are plotted opposite. It can be seen that the currents under Strategy I are not obviously affected by the switching operations beside some fast transients after on and off instances. Because the DC/DC converters of Strategy I cannot control power flow through them, they act only as DC voltage balancers. Therefore, the power flow of each DC sub-system under Strategy I can change automatically.

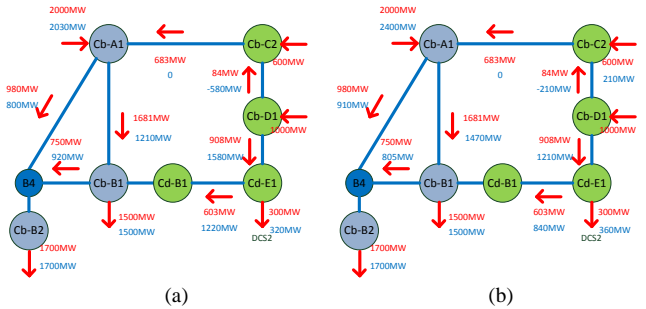


Fig 9. Power flow after switching cable A1-C2: (a) Strategy I, (b) Strategy II. The red color stands for original data and the dark blue color for the post-switching data; the red arrow represents reference direction.

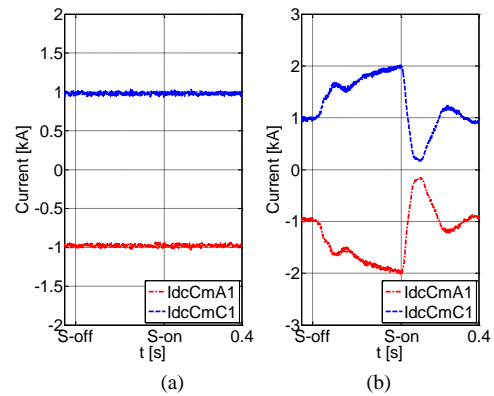


Fig 10. Comparison of strategies on DC currents of DCS1: (a) Strategy I, (b)Strategy II

On a contrary, DCS1 and DCS3 are sensitive under Strategy II. It can be seen that the current (power) injected from Cm-C1 increases while that from Cb-C2 decreases, as it

demonstrates in Fig.10(b) and Fig.11(b) respectively. This results from the suppression of DC/DC converter Cd-B1 in active power and the incapability of Cm-C1 on power control; the energy is delivered to DCS1 through Cm-C1, what is more, the power gap is compensated by converter Cb-A1, which can be proved by Fig.9(b) and Fig.11(b). Therefore, DCS2 can still work around pre-switching state according to Fig.12. It has been observed that the DC voltage of HV side (V_m) of DC/DC converter climbs to approximately 1.125pu after switch-off. However, the voltage of LV side (V_c) can still maintain the rated level because of the decreasing of the duty ratio declines, which is depicted in Fig.13.

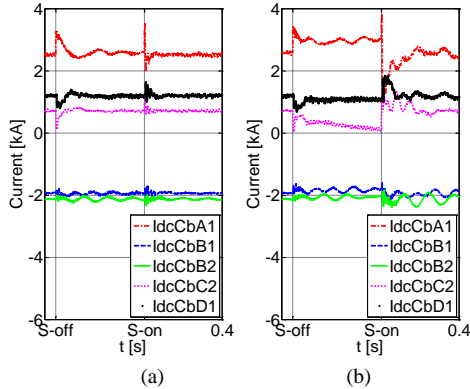


Fig 11. Comparison of strategies on DC currents of DCS3: (a) Strategy I, (b) Strategy II

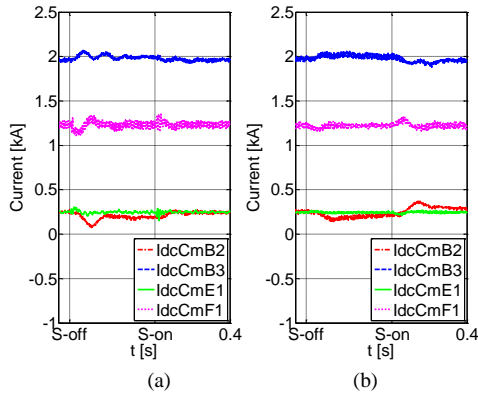


Fig 12. Comparison of strategies on DC currents of DCS2: (a) Strategy I, (b) Strategy II

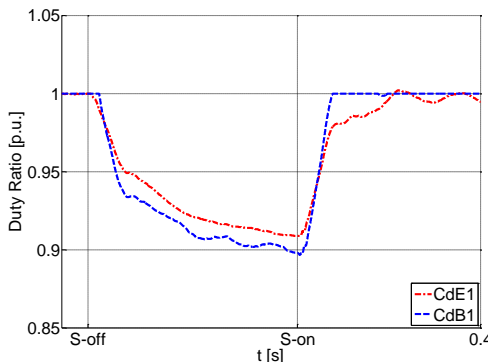


Fig 13. The duty ratios of DC/DC converter CdE1 and CdB1 under Strategy II

From the presented simulation results, it is obvious that Strategy I is much more robust against disturbances on the

network than Strategy II; the rehabilitation is faster after fault and all the converters can still operate around their original set points if a cable is switched off. These advantages are realized by sufficient redundancy in control, as each converter plays a role in regulating DC network, and the ‘ideal’ DC/DC converters. The Strategy II is more realistic on DC/DC converter side. Although the DC voltage of HV side may exceed upper limit, the LV side can still maintain rated level voltage, which means that the DC/DC converter can prevent healthy part of the whole system from disturbances.

C. Regulation of DC/DC Converter

As mentioned above, the DC/DC converter can prevent fault from spreading to healthy parts of the whole network under certain strategy, a simulation of fault on the terminal of DC/DC converter (the LV side of Cd-B1) is also performed. The fault is applied at 0.02s.

As mentioned before, the DC/DC converter is modeled with ideal transformer in Strategy I, which means there is no controllability at the DC/DC converter. Thus, it can be observed that the DC fault propagates from DCS3 to DCS2. However, when it comes to Strategy II, the DC fault can be isolated from DCS2. The simulation results are shown in Fig.14, please note the frame of dc current. Therefore, DC faults happening under Strategy I may cause malfunction of protection in the healthy regions. From another point of view, if the protection of a MTDC system cannot meet the requirement of selectivity, it is advisable to use DC/DC converters at crucial points to offer necessary protective function. At the meantime, the type of DC/DC converter plays a crucial role here, as both the coupled topology and control method influence network behavior.

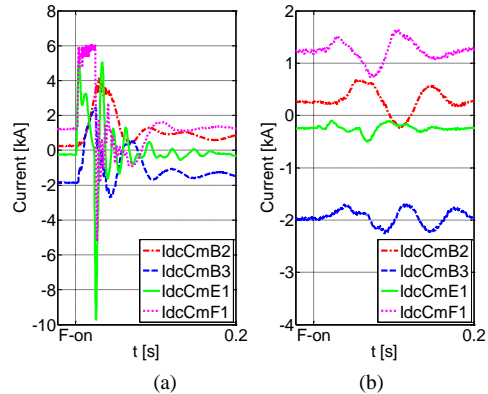


Fig 14. Comparison of currents of DCS2 after DC fault on DC/DC converter terminal: (a) Strategy I, (b) Strategy II

V. CONCLUSIONS

Transient studies are important for protection design, which needs to operate in around 10ms after the fault occurrence. The simulations are an evaluation of the network responses when coping with different kinds of disturbances. Because of different strategies, the elements of network have to be changed either in modelling method or control modes for specific operation purposes, i.e. the generators are changed from voltage source to fixed power source when applying

Strategy II. This paper analyses the influences of these changes on the transient behaviors of MTDC system. According to the simulation results, Strategy I is a suitable one for protection study as it has a higher level of control margin. Additionally, with it, the converter can restore DC voltage quickly, which is beneficial for post-fault recovery. On the other hand, Strategy II could be applied as an alternative strategy either to test the protection selectivity or to improve the fault detection and location algorithms, as the disturbances may cause malfunction of protective devices.

In the next stage, the more dedicated controlling study will be conducted with established strategies. Improved control methods will be proposed accordingly. Specifically, it has been found that large valued current flows through semi-conductors when DC fault happens, thus new VSC topology is under design and will be adopted with chosen strategies.

VI. REFERENCES

- [1] B. T. Ooi and X. Wang, "Voltage Angle Lock Loop Control of Boost Type PWM Converter for HVDC Application," *IEEE Transactions on Power Electronics*, vol. 5, pp. 229-235, 1990.
- [2] B. T. Ooi and X. Wang, "Boost type PWM-HVDC Transmission System," *IEEE Transactions of Power Delivery*, vol. 5, pp. 1557-1563, 1991.
- [3] G. Asplund, K. Eriksson and K. Sevansson, "DC Transmission based on Voltage Source Converters," in *CIGRE SC14 Colloquium*, South Africa, 1997.
- [4] T. Nakjima, "Field Testing of 53 MVA Three-Terminal DC Link between Power Systems Using GTO Converters," in *International Power Electronics Conference*, Tokyo, 2000.
- [5] F. Schettler, H. Huang and N. Christl, "HVDC Transmission System using Voltage Sourced Converters-Design and Applications," in *IEEE PES Summer Meeting*, 2000.
- [6] D. Jovicic, D. Van Hertem, K. Linden, J.-P. Taisne and W. Grieshaber, "Feasibility of DC transmission networks," in *Innovative Smart Grid Technologies (ISGT Europe), 2011 2nd IEEE PES International Conference and Exhibition on*, Manchester, 2011.
- [7] L. Tang and B. T. Ooi, "Protection of VSC-multi-terminal HVDC against DC faults," in *Power Electronics Specialists Conference, 2002. pesc 02. 2002 IEEE 33rd Annual*, 2002.
- [8] F. Deng and Z. Chen, "Design of Protection Inductors for HVDC Transmission Line Within DC Grid Offshore Wind Farms," *IEEE Transactions on Power Delivery*, vol. 28, no. 1, pp. 75-83, 2013.
- [9] J. Yang, J. E. Fletcher and J. O'Reilly, "Multiterminal DC Wind Farm Collection Grid Internal Fault Analysis and Protection Design," *IEEE Transaction on Power Delivery*, vol. 25, no. 4, pp. 2308-2318, 2010.
- [10] K. Han, Z. Cai and Y. Liu, "Study on Protective Performance of HVDC Transmission Line Protection with Different Types of Line Fault," in *Electric Utility Deregulation and Restructuring and Power Technologies (DRPT), 2011 4th International Conference on*, 2011.
- [11] J. Suonan, J. Zhang, J. Zaibin, Y. Liming and S. Guobing, "Distance Protection for HVDC Transmission Lines Considering Frequency-Dependant Parameters," *IEEE Transactions on Power Delivery*, vol. 28, no. 2, pp. 723-732, 2013.
- [12] B4-57 and B4-58, "The Cigre B4 DC Grid Test System," CIGRE WG B4.
Available:http://b4.cigre.org/content/download/34038/1483266/version/1/file/cigre_b4_dc_grid_test_system_final_corrected_version_with_intr_o_v15.docx
- [13] U. N. Gnanarathna, A. M. Gole and R. P. Jayasinghe, "Efficient Modeling of Modular Multilevel HVDC Converters (MMC) on Electromagnetic Transient Simulation Programs," *IEEE Transactions on Power Delivery*, vol. 26, no. 1, pp. 316-324, 2011.
- [14] A. Lindberg, "PWM and Control of Two and Three level High Power Voltage Source Converter," Licentiate Thesis, Royal Institute of Technology, Stockholm, Sweden, 1995.
- [15] J. Peralta, H. Saad, S. Denetiere and J. Mahseredjian, "Detailed and Averaged Models for a 401-level MMC- HVDC System," *IEEE Transactions on Power Delivery*, vol. 27, no. 3, pp. 1501-1508, 2012.
- [16] "PSCAD X4 Online Help," Manitoba HVDC Research Centre, Manitoba, Canada, 2013.
- [17] F. Mura, C. Meyer and R. W. De Doncker, "Stability Analysis of High-Power DC Grids," *IEEE Trans. Industry Applications*, vol. 46, no. 2, pp. 584-592, May, 2010.